Creep Fatigue Interaction on Small Mock-up Submitted to Thermal Shocks and Primary Stresses

M.T. Cabrillat, J.L. Carbonnier

C.E.A., CEN Cadarache, DRNR/STRA, B.P. No. 1, F-13115 St. Paul-lez-Durance, France

G. Cordier

Electricité de France, SEPTEN, 12-14 av. Dutrievoz, F-69628 Villeurbanne Cedex, France

Abstract

An experimental program has been undertaken on small structures to study creep-fatigue interaction in the presence of stress and strain fields similar to those supported by structures in LMFBR. Small mock-ups are loaded with load-controlled stresses and submitted to sodium thermal shocks. The program is currently in progress. This paper describes the test principles and the first experimental results, together with the first creep-fatigue damage evaluation.

1 Introduction

Assessing creep-fatigue damage on structures subjected to high-temperature operation in sodium still involves considerable uncertainties, not the least of which is that all of the laws used are based on uniaxial tests, generally conducted in air.

Uniaxial tests don't allow to study load-controlled and strain-controlled stresses interaction. Tests on small mock-ups are necessary to evaluate the cumulated damage due to load-controlled stresses creep and strain-controlled stresses relaxation.

That's the purpose of the experimental program presented in this paper.

Tests are realized in sodium. The mock-ups are subjected to a permanent load and to thermal shocks. Their shape has been determined in order to have stress and strains fields similar to those found in actual structures and especially to study multiaxial stresses influence. Sodium is used as the test medium to produce thermal transients similar to those sustained by reactor structures .

2 Current Analysis Methods

Creep-fatigue damage is evaluated in a different way according to the design codes :

- For code case N47 life reduction associated with slow strain rates and hold times is taken into account in the fatigue curve T 1430 : relaxation of peak stresses is included in fatigue damage.

Creep damage due to primary stresses and to secondary stresses (elastic follow up) is calculated separately.

- In RCC-MR code fatigue damage is evaluated on a fatigue curve which does not include hold time effect, and creep damage is calculated using the stress :

$\sigma_k = \text{Moy}\ \overline{P} + K_s\ \overline{\Delta\sigma}^*$ which takes into account primary, secondary and peak stresses, and evaluates the maximum total stress during the cycle.

- . Moy $\overline{P}$ is the mean equivalent primary stress value during the cycle
- . $\overline{\Delta\sigma}^*$ is the ordinate on the cyclic stress-strain curve corresponding to the abscissa $\Delta\varepsilon_T$ (strain range used to evaluate fatigue damage)
- . K_s is a cycle symmetry correction coefficient.

These two methods are generally thought to be too much conservative. Experimental tests are necessary to evaluate conservatism of these methods and to improve creep-fatigue evaluation in complex loading cases.

3 Test Conditions

Tests are realized in sodium on small structures . These mock-ups are set into a 1080 mm diameter vessel. Their small size allow to put four of them together in the vessel.
A test facility scheme is shown on fig.5.

3.1 Test Specimens

The test specimens represent a shell-to-plate junction (Figure 1). They include a geometrical discontinuity to obtain stress and strain concentrations in these areas. Two types of specimens are used : under axial loading only membrane stresses will be exerted in specimen 1, while major bending stresses will occur in specimen 2.

3.2 Stress Loading

The specimens are subjected to a permanent primary stress loading and to thermal shocks. The specimen is maintained at a temperature of 600°C by internal heating, and cold shocks are produced every 6 hours by exposing the outer face of the specimen to cooler (400°C) sodium. The shock lasts for 20 seconds, after which the specimen temperature rises again to 600°C over a period of about 10 minutes. The primary loading is an axial stress applied by means of a jack.

Figures 2 and 3 show the stresses sustained by the two specimens under the effects of the primary stress load in one case, and during the thermal shock in the other. During hold times the residual stresses state is as shown in Figure 4.

Four series of test are planned for each type of specimen, according to the primary stress values, thermal loading staying always the same :

- thermal shocks under a primary stress equal to the mean yielding stress : P= 140 MPa
- thermal shocks under a primary stress about Sm value : 100 MPa
- thermal shocks under a primary stress of 50 MPa
- thermal shocks under a low primary stress : P = 20 MPa

Moreover a creep test under a high primary stress : P = 200 - 240 MPa is realized in air at 600°C . Every test is performed twice.

4 Calculations

4.1 Thermal Calculations

Thermocouples are installed to monitor the temperature variations, and subsequently to determine the temperature fields in the specimens during the thermal transients.
Calculations are conducted using a heat exchange coefficient of 20.000 w/m² °C on the outer skin of the sample, and taking into account the sodium conductivity inside the sample. The results are in good agreement with measurements. (Fig.6)

4.2 Mechanical Calculations

Various calculations were performed to estimate the creep-fatigue life of these specimens. At the present time, the results are available only for specimen 1. The following calculations were performed :
- elastic analysis,
- plastic analysis with a linear kinematic hardening model identified on the reduced cyclic curve at 600°C. (E = 145000 MPa, h = 32800 MPa, Sy = 180 MPa)

These calculations were performed for the four primary stress levels.

4.2-1 Elastic Analysis

Maximum stress loading occurred on the shell in the leadout portion of the groove-ring, with a maximum stress of 771.8 MPa recorded 1.5 sec after the beginning of the transient. Based on RCC-MR analysis, $\Delta\varepsilon_T$ = 0.666% and therefore N = 260 allowable cycles on the design curve.

Creep damage is estimated from the stress loading :

$$\sigma_k = \text{Moy}\ \overline{P} + ks\ \overline{\Delta\sigma}^*$$

The following results were obtained for the different primary stress values :

Stress Loading MPa	σ= 0	σ= 20	σ= 50	σ= 100	σ= 140
σK (MPa)	255	275	305	355	395
Ta (h)	20	9	2	<1	<1
Fatigue-Creep Life (number of cycles)	3c D_F=0 D_C=1	2c D_F=0 D_C=1	1c D_F=0 D_C=1	1c D_F=0 D_C=1	1c D_F=0 D_C=1

The results are based on design curves, and are thus assigned a safety factor.

This safety factor can be suppressed by evaluating damage fatigue using the best fit curve and creep damage using the mean stress-to rupture curve and without the coefficient 0.9 on this stress.

Doing that, the following results are obtained :

Stress Loading MPa	σ= 0	σ= 20	σ= 50	σ= 100	σ= 140
Fatigue-Creep Life (cycles)	65c D_F=0.01 D_C=0.98	40c D_F=0 D_C=1	13c D_F=0 D_C=1	3c D_F=0 D_C=1	1c D_F=0 D_C=1

4.2-2 Plastic Analysis : Linear Kinematic Model Identified on the Reduced Cyclic Curve.

Plastic calculations were performed for each primary stress level. Figure 7 shows the (σvM, εvM) cycles obtained at the most heavily loaded point (i.e. inside the groove-ring). It may be noted that similar cycles are always obtained, and that the primary stress effect results in a cycle shift.

Fatigue damage will thus be the same in all cases. Creep damage, on the other hand, is related to the stress level at the beginning of the holding time, and will thus vary considerably depending on the stress loading conditions.

The fatigue-creep analysis gives the following results :

$\Delta\varepsilon_T$ = 0.584%, i.e. N = 360 cycles.

Stress Loading MPa	σ = 0	σ= 20	σ= 50	σ= 100	σ= 140
σvM at beginning of hold time MPa	120.8	137.8	164.7	218.8	258.7
Fatigue-Creep life (design curve) number of cycles	240c D_F=0.67 D_C=0.14	160c D_F=0.44 D_C=0.24	80c D_F=0.22 D_C=0.48	12c D_F=0.03 D_C=0.9	3c D_F=0 D_C=1
Fatigue-Creep life (w/O safety factor) number of cycles	3100c D_F=0.43 D_C=0.23	1900c D_F=0.26 D_C=0.38	1080c D_F=0.15 D_C=0.65	230c D_F=0.03 D_C=0.92	65c D_F=0.01 D_C=0.98

It can clearly be seen that the creep damage increases relative to the fatigue damage as the primary stress value rises.

Other plastic and viscoplastic calculations are planned to test influence and validity of different models in such cases of complex loading.

5 Experimental Results

Testing has been completed on a first series of specimens with a primary stress loading of 140 MPa. After about 60 cycles it was observed that three out of four specimens appeared to be cracked. Conventional crack detection methods gave negative results. Only ultrasonic examination yielded indications corresponding to flaws on the specimen inner surface.

Destructive examination revealed incipient cracking (Figure 8). These cracks appear to be characteristic of fatigue-creep phenomena : grain decoherence is observed together with fatigue striations.

These examinations will be continued in order to characterize the cracks.

6 Conclusion

The first results of this program are :

- a good working of the test facility
- a good agreement between thermal calculations and measurements
- failure have been obtained, and first examinations show , as expected, a preponderant creep damage.

Therefore this program should allow to evaluate validity of current analysis methods and to improve them :

for elastic analysis with a better evaluation of the interaction between creep damage of primary stresses and relaxation damage of secondary and peak stresses, and for inelastic analysis with qualification of different plastic and viscoplastic material behaviour models and damage models.

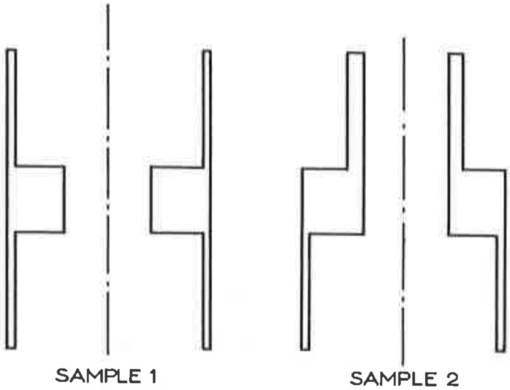

figure 1

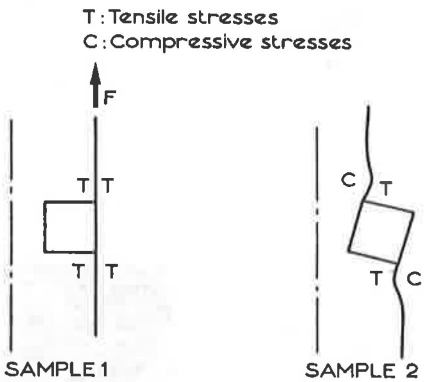

STRESSES DUE TO AXIAL LOAD
figure 2

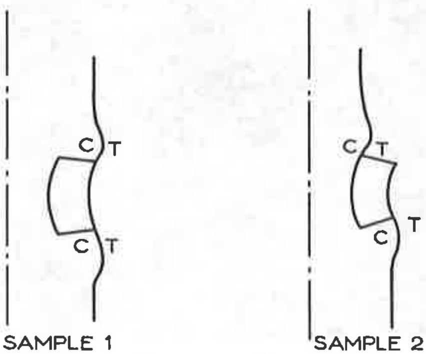

DEFORMATION AT THE BEGINNING OF THERMAL SHOCK
figure 3

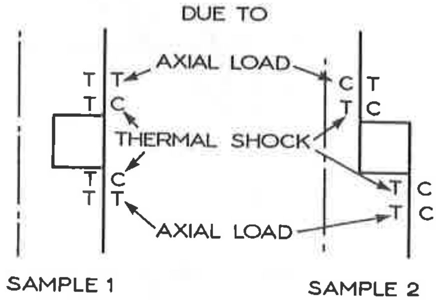

RESIDUAL STRESSES DURING HOLD TIME
figure 4

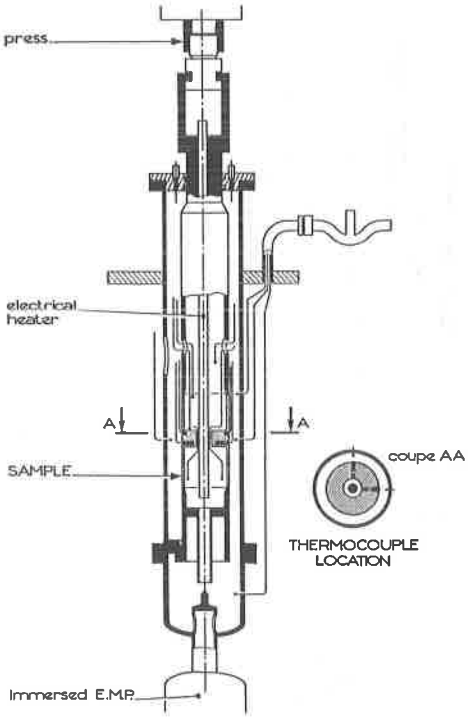

Fig.5: test facility

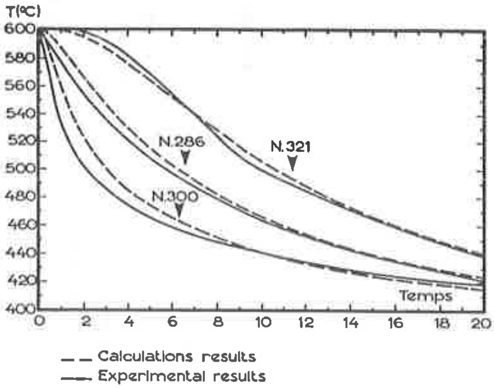

Fig.6: comparison between calculations and experimental measurements

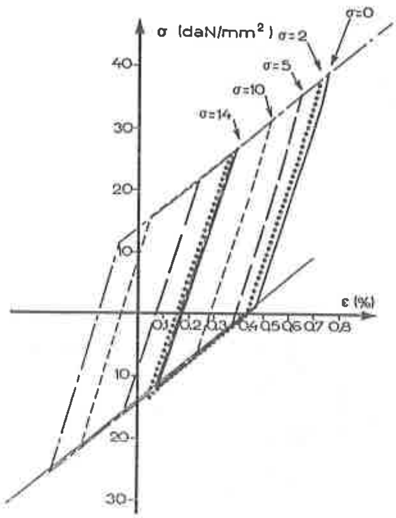

Fig.7: linear kinematic model (σ-ε) cycles for the different loading cases

Fig.8: view of the cracks